ISET Journal of Earthquake Technology, Paper No. 382, Vol. 35, No. 4, December 1998, pp. 185-206

PASSIVE FLUID VISCOUS DAMPING SYSTEMS FOR SEISMIC ENERGY DISSIPATION

M. D. Symans* and M. C. Constantinou**

*Assistant Professor, Dept. of Civil and Env. Eng., Washington State University, Pullman, WA 99164-2910, USA
**Professor, Dept. of Civil Engineering, State University of New York at Buffalo, Buffalo, NY, 14228, USA

ABSTRACT

Passive fluid viscous damping systems are generally well suited to vibration control of civil structures subjected to seismic excitation. In particular, fluid viscous dampers that operate on the principle of fluid orificing exhibit extraordinarily high levels of energy dissipation density. Such dampers are the primary focus of this paper. The dynamic behavior of a fluid orificing damper is examined through steady-state cyclic test data. Mathematical models of the damper are derived from the cyclic test data and subsequently used in obtaining analytical predictions of the seismic response of a scale-model building structure subjected to earthquake ground acceleration. The discussion on fluid orificing dampers is expanded by considering a generalized mathematical model for describing both linear and nonlinear fluid viscous damper behavior. The energy dissipation characteristics of generalized fluid viscous dampers are then examined with reference to the performance of an idealized single-story structure. Finally, a discussion of current applications of fluid viscous dampers for seismic protection of building and bridge structures is presented.

KEYWORDS: Energy Dissipation, Fluid Viscous Damping, Passive Control, Seismic Testing, Seismic Protection

INTRODUCTION

Many methods have been proposed for mitigating the harmful effects of strong earthquakes. The conventional approach requires that structures passively resist earthquakes through a combination of strength, deformability, and energy absorption. The level of damping in these structures is typically very low and therefore the amount of energy dissipated during elastic behavior is very low. During strong earthquakes, these structures deform well beyond the elastic limit and remain intact due to their ability to deform inelastically. The inelastic deformation takes the form of localized plastic hinges which results in increased flexibility and energy dissipation. Therefore, much of the earthquake energy is absorbed by the structure through localized damage of the lateral force resisting system.

An alternate approach to mitigating the hazardous effects of earthquakes is based on a consideration of the distribution of energy within a structure. During a seismic event, the input energy from the ground acceleration is transformed into both kinetic and potential (strain) energy which must be either absorbed or dissipated through heat. The inherent energy dissipation capacity of the structure will eventually withdraw all of the seismic input energy from the structure. However, for strong earthquakes a large portion of the input energy will be absorbed by hysteretic action (i.e., damage to the structure). Rather than relying on structural damage to dissipate the seismic energy, one may append a supplemental energy dissipation system to the structure so as to reduce the energy dissipation demand on the structure itself. This approach to seismic energy dissipation is made clear by considering the following time-dependent conservation of energy relationship (Uang and Bertero, 1990)

$$E(t) = E_k(t) + E_s(t) + E_h(t) + E_d(t) \tag{1}$$

where E is the absolute energy input from the earthquake motion, E_k is the absolute kinetic energy, E_s is the elastic (recoverable) strain energy, E_h is the irrecoverable energy dissipated by the structural system through inelastic or other forms of action (e.g., viscous and hysteretic), E_d is the energy dissipated by a supplemental damping system, and t represents time. The absolute energy input, E,

represents the work done by the total base shear force at the foundation on the ground (foundation) displacement and thus accounts for the effect of the inertia forces on the structure.

In the conventional design approach, the term E_d in Equation (1) is not present. In this case, acceptable structural performance is accomplished by the occurrence of inelastic deformations, which has the direct effect of increasing E_h. It also has an indirect effect. The occurrence of inelastic deformations results in softening of the structural system which itself modifies the absolute input energy. In effect, the increased flexibility acts as a filter, which reflects a portion of the earthquake energy.

An alternate approach to improving the seismic response of structures involves the inclusion of supplemental energy dissipation systems in the structure. In this case, the term E_d in Equation (1) is present and accounts for a major portion of the seismic energy that is absorbed during the earthquake. In general, the presence of supplemental dampers affects all of the terms in Equation (1) as will be explained in more detail later in this paper. In a supplemental energy dissipation system, mechanical devices are either incorporated in the frame of the structure or within a base isolation system. There are a variety of devices available for dissipating seismic energy including hysteretic (displacement-dependent) dampers, friction dampers, viscoelastic solid dampers, and viscoelastic fluid dampers. This paper concentrates on the use of fluid dampers as elements of a supplemental seismic energy dissipation system.

FLUID DAMPERS FOR SEISMIC ENERGY DISSIPATION

There are essentially two different design approaches for using fluids to dissipate seismic energy. One straightforward approach is patterned directly after the classical dashpot. In this case, energy dissipation occurs via conversion of mechanical energy to heat as a piston deforms a thick, highly viscous substance, such as a silicone gel. Figure 1 depicts one such damper, which has found application as a component in seismic base isolation systems (Huffmann, 1985; Makris and Constantinou, 1990). While these devices could also be deployed within the superstructure, an alternative, and perhaps more effective, design concept involves the development of the viscous damping wall illustrated in Figure 2 (Arima et al., 1988). In this design, the piston is simply a steel plate constrained to move in its plane within a narrow rectangular steel container filled with a viscous fluid. For typical installation in a frame bay, the piston is attached to the upper floor, while the container is fixed to the lower floor. Relative interstory motion shears the fluid and thus provides energy dissipation.

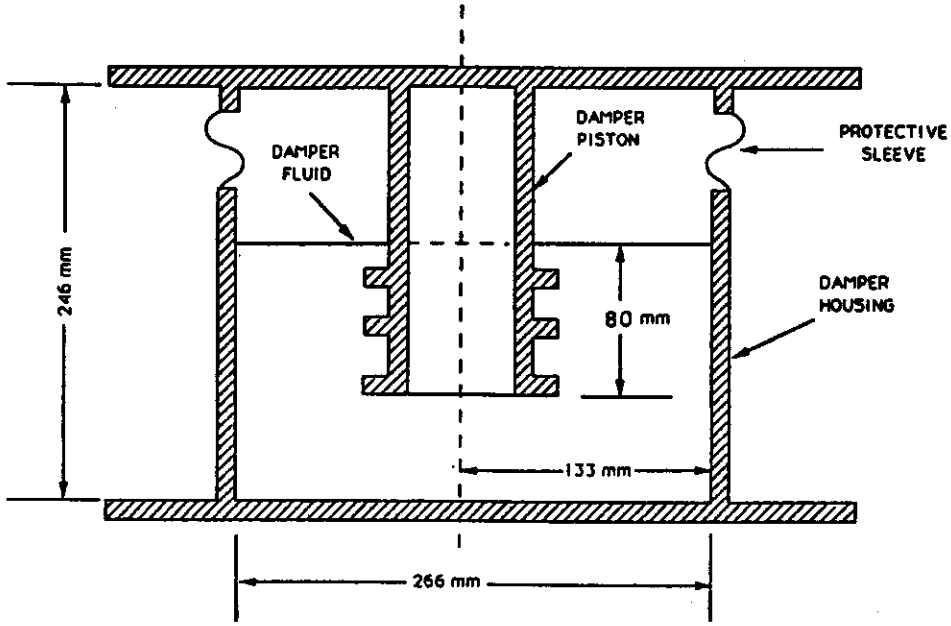

Fig. 1 Cross-section of cylindrical pot viscoelastic fluid damper
(adapted from Makris and Constantinou 1990)

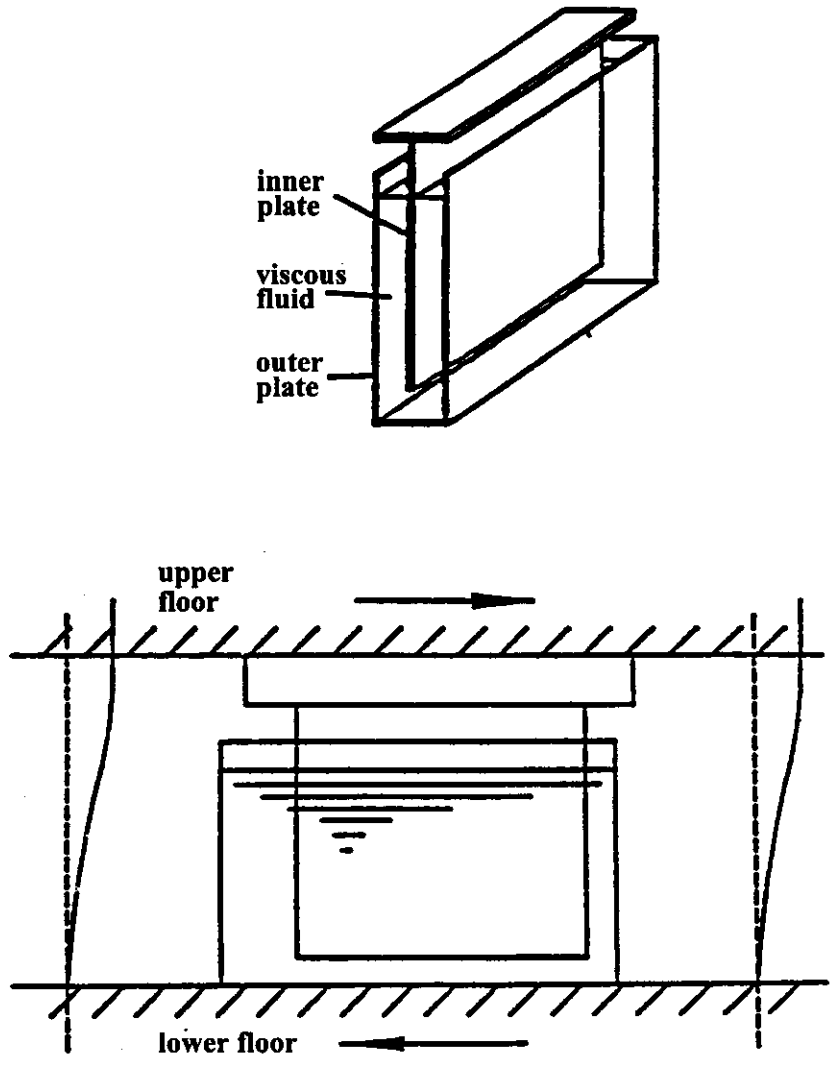

Fig. 2 Viscous damping wall (adapted from Arima et al., 1988)

Both of the devices discussed above accomplish their objectives through the deformation of a viscous fluid residing in an open container. In order to maximize the energy dissipation density of these devices, one must employ materials with large viscosities. Typically, this leads to the selection of materials that exhibit both frequency and temperature dependent behavior. There is, however, another class of fluid dampers that rely instead upon the flow of fluids within a closed container. In these designs, the piston acts now, not simply to deform the fluid locally, but rather, to force the fluid to pass through small orifices. As a result, extremely high levels of energy dissipation density are possible. However, a correspondingly high level of sophistication is required for proper internal design of the damper unit.

Fluid dampers which operate on the principle of fluid flow through orifices were originally developed for the shock isolation of military hardware. To appreciate the level of technology involved in these shock isolation systems, note that the so-called weapons grade shock usually has free field input wave forms with peak velocities in excess of 4500 mm/sec, rise times of less than 2 msec and peak accelerations on the order of 200 g (Clements, 1972). The particular fluid damper that was the focus of the research described herein originated in a classified application on the U.S. Air Force B-2 Stealth Bomber. Thus, the device includes performance characteristics considered as state-of-the-art in hydraulic technology. Two of these characteristics which are of particular interest in seismic hazard mitigation applications are essentially linear viscous behavior and capability of operating with stable mechanical properties over a wide ambient temperature range.

DESCRIPTION AND BEHAVIOR OF TESTED FLUID DAMPERS

The construction of the fluid dampers tested by Constantinou and Symans (1993a and 1992) is shown in Figure 3. The damper had a maximum force output of 450 N, a stroke of ±51 mm, a length of 280 mm and weighed 10 N. The damper consists of a stainless steel piston with a bronze orifice head and a piston rod make-up accumulator. The damper is filled with a thin silicone oil having a kinematic viscosity of 100 cSt. High strength seals are utilized to maintain closure over the design life of the damper. The piston head orifices are designed such that the fluid flow is altered according to the fluid speed resulting in a force output which is essentially proportional to the relative velocity of the piston head with respect to the damper housing. Such orifices are known as fluidic control orifices, fluidic coming from the concatenation of fluid and logic (i.e., logical operations using fluids).

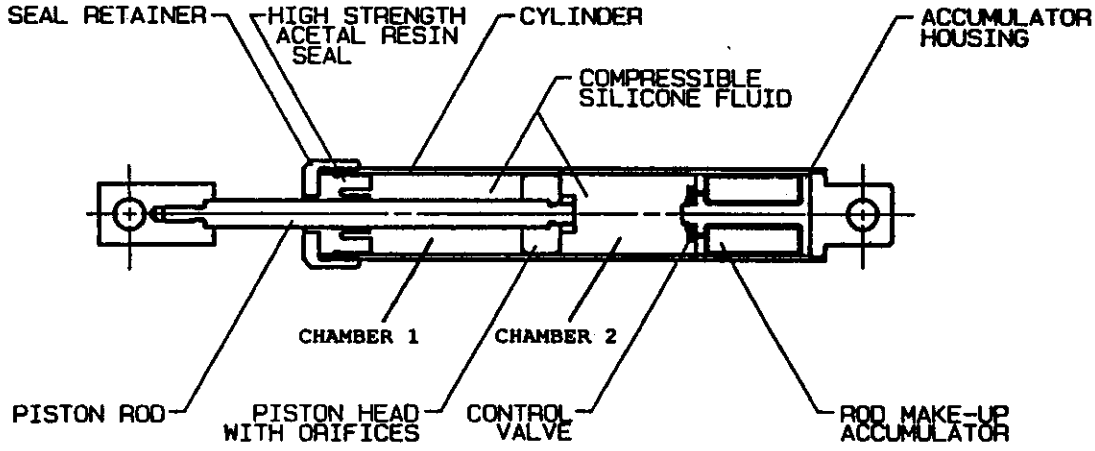

Fig. 3 Construction of tested fluid damper

The force generated by the damper is a result of a pressure differential across the piston head. When the damper is subjected to a compressive force, the fluid volume is reduced by the product of travel and piston rod area. Since the fluid is nearly incompressible, the reduction in fluid volume results in the development of a restoring force. This is prevented by the use of a rod make-up accumulator and control valve. An alternate construction of this device is with a run-through rod in which the rod enters the damper, is connected to the piston head, and then continues out through the opposite end of the damper. This arrangement avoids changes in fluid volume and therefore prevents the development of a restoring force. The construction of large size dampers for structural control applications typically includes a run-through rod rather than an accumulator.

The flow of fluid through the piston head orifices is compensated according to the temperature such that the mechanical properties remain relatively stable over a wide temperature range (–40°C to 70°C). This is accomplished passively through the use of an orifice design which utilizes a bi-metallic thermostat. Note that the dampers may be described as "inertial" dampers since the behavior is primarily governed by the speed of fluid through the orifices and secondarily by the mechanical properties of the fluid. Therefore, any effect of temperature on the fluid viscosity will not significantly alter the behavior of the damper.

The mechanical properties of the dampers were determined by subjecting them to steady-state cyclic motion at various frequency levels and ambient temperature conditions. Typical recorded force-displacement loops for sinusoidal input motion are presented in Figure 4 for room temperature conditions (23°C) and frequencies of 1, 2 and 4 Hz. In this range of frequencies, the device exhibits insignificant storage stiffness and its behavior is essentially linear viscous. At frequencies above about 4 Hz (the so-called cut-off frequency), the damper exhibited storage stiffness which reached values approximately equal to the loss stiffness at frequencies exceeding 20 Hz. In general, the value of the cut-off frequency depends on the design of the accumulator and may be specified in the design. The existence of the aforementioned cut-off frequency is a desirable property. In the case where the dampers are installed within the framing of a structure, the dampers may provide additional viscous type damping

to the fundamental mode of the structure (typically with a natural frequency less than the cut-off frequency) and additional damping and stiffness to the higher modes. This may, in effect, completely suppress the contribution of the higher modes of vibration.

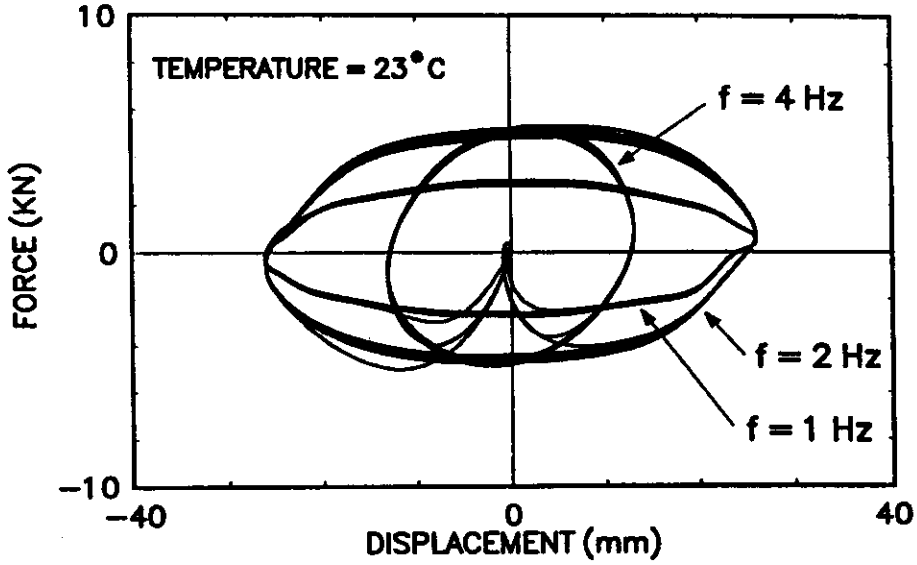

Fig. 4 Recorded force-displacement loops for three different harmonic motions

MATHEMATICAL MODELS FOR FLUID DAMPER BEHAVIOR

Based on the experimental results described above, it is apparent that over a large frequency range, the tested dampers exhibit viscoelastic fluid behavior. The simplest model to account for this behavior is the Maxwell model (Bird et al., 1987). The Maxwell model may be described at the macroscopic level as follows

$$P(t) + \lambda \dot{P}(t) = C_o \dot{u}(t) \tag{2}$$

where P is the damper output force, λ is the relaxation time, C_o is the damping constant at zero frequency, u is the displacement of the piston head with respect to the damper housing, and the overdot indicates first-order differentiation with respect to time. For identification of the damper behavior, the classical Maxwell model of Equation (2) was generalized to the following form in which the derivatives are of fractional order (Makris and Constantinou, 1991)

$$P(t) + \lambda D^r[P(t)] = C_o D^q[u(t)] \tag{3}$$

where $D^r[\bullet]$ and $D^q[\bullet]$ are fractional derivatives of order r and q, respectively, of the contained time-dependent functions. For complex viscoelastic fluid behavior, the fractional derivative model typically offers an improved ability to describe the damper behavior over a wide frequency range. Other more advanced models of viscoelasticity have been examined for modeling the dynamic behavior of fluid dampers. For example, Makris and Constantinou (1993) have modeled the dynamic behavior of a fluid damper using viscoelastic models in which the order of the time derivatives and the coefficients of the model are complex-valued. The resulting models may be regarded as generalized forms of linear models of viscoelasticity.

1. Calibration of Mathematical Model

The calibration of the model of Equation (3) was performed for the case of room temperature for which experimental data over a wide frequency range were available. The calibration resulted in parameters r =1, q =1, λ = 6 msec and C_o = 15.45 N-sec/mm. Interestingly, the calibrated model can be represented by the classical Maxwell model of Equation (2). A comparison of experimental and analytically derived properties of damping coefficient and storage stiffness is presented in Figure 5. The

comparison is very good except for frequencies above 20 Hz, where the model underpredicts the storage stiffness. Such frequencies are typically not considered in seismic analysis. Further, the model predicts nonzero storage stiffness in the low frequency range (less than about 2 Hz). However, the predicted storage stiffness is insignificant for practical purposes.

The damper exhibits a relaxation time of only 6 msec, indicating that for low rates of damper force, the term $\lambda \dot{P}$ in Equation (2) is insignificant. This occurs for frequencies below the cut-off frequency of 4 Hz. Accordingly, for typical structural applications, the term $\lambda \dot{P}$ may be neglected. Thus, the model of the damper for frequencies of motion below the cut-off frequency is simply

$$P(t) = C_o \dot{u}(t) \tag{4}$$

and, therefore, for most practical purposes, the damper behaves as a linear viscous dashpot.

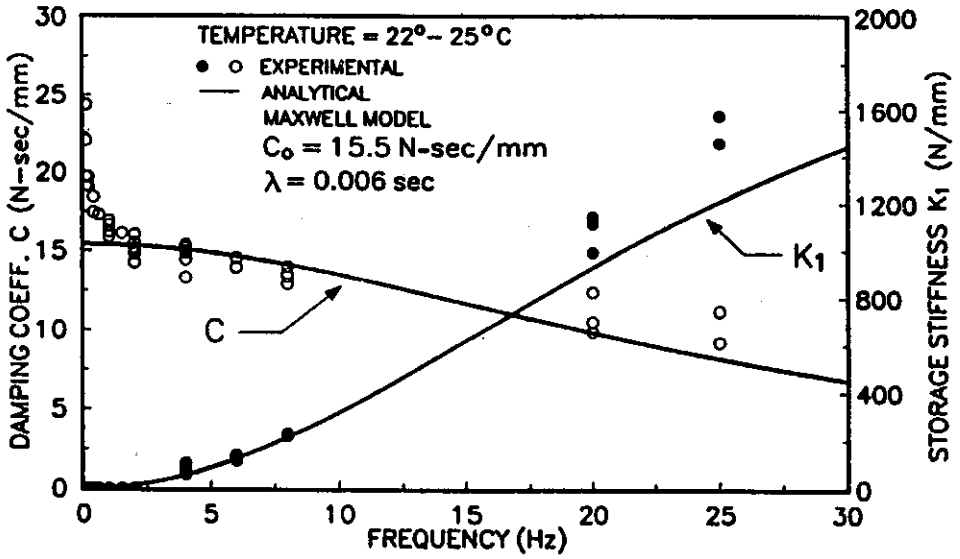

Fig. 5 Comparison of experimental and analytically-derived values of damping coefficient and storage stiffness

The frequency dependencies described above result from the use of accumulators or similar parts that involve the operation of valves. Valves themselves have dynamic characteristics and typically may not be compatible with the dynamic movement of the damper piston rod at high frequency. This results in restricted fluid flow to the accumulator and, thus, reduction in fluid volume. If desired, this phenomenon can be entirely prevented via the use of a run-through rod as described previously in Section 3.

2. Temperature Effects

The effect that temperature has on the single parameter, C_o, of the linear viscous dashpot model given by Equation (4) is shown in Figure 6. The recorded peak force in each test is plotted against the imposed peak velocity for three ambient temperature conditions. The data is separated into two sets, one for frequencies of motion less than 5 Hz and the other for frequencies above 5 Hz. It may be seen that the experimental results may be fitted with straight lines having slope equal to C_o. For room temperature (24°C) and above, the behavior is essentially linear viscous to velocities of about 500 mm/sec and beyond. As temperature drops, the experimental results deviate from linearity at a lower velocity. The values of the constant C_o in Figure 6 demonstrate that the damper exhibits stable behavior over a wide range of temperatures. Between about 0°C and 50°C, the constant C_o reduces by a factor of less than 2. Assuming that a design for a building application will be anchored at a temperature of about 24°C, variations of temperature in the range of 0°C to 50°C will result in variations of the damping ratio

of +44 % to −25 %. That is, if a design calls for a damping ratio of 20 %, extreme temperature variations will alter the damping ratio in the range of 15 % to 29 %. This rather small change in properties over a wide range of temperatures is in sharp contrast to the extreme temperature dependency of viscoelastic solid dampers (Constantinou and Symans, 1993b).

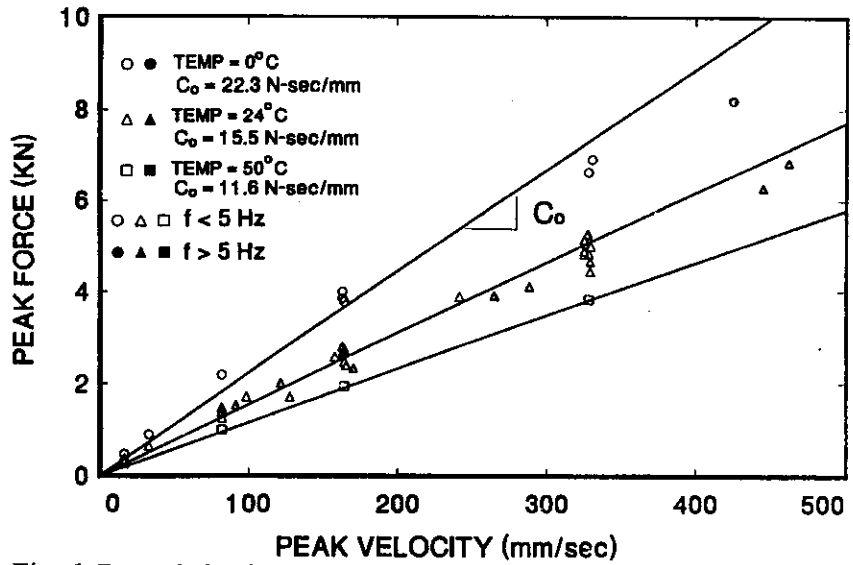

Fig. 6 Recorded values of peak force versus peak velocity for a range of ambient temperature levels

The issue of viscous heating in passive fluid dampers has recently been examined analytically by Makris et al. (1998). The fluid temperature increase per cycle of steady-state harmonic motion was shown to be quite significant in the case of long-stroke motions such as may be expected in seismic isolation applications. Specifically, it was shown that the temperature rise for long-stroke motions is proportional to the pressure drop and independent of the amplitude of the piston head velocity. In cases where viscous heating is a concern, the pressure drop within the damper should be reduced by utilizing piston heads with large diameters.

SEISMIC SIMULATION TESTING

A series of earthquake simulation tests were performed on a 1:4 scale three-story steel moment-resisting frame as shown in Figure 7. The total weight of the three-story model building was 28 kN, equally distributed to each floor and the total height of the frame was about 2.5 m.. The structure was tested both in a one-story and three-story configuration. In the one-story configuration, the upper two stories were rigidly braced and either two or four dampers were placed in the diagonal bracing of the first story. In the three-story configuration, seismic tests were performed with two, four or six dampers within the diagonal bracing system as shown in Figure 7. The dynamic characteristics of the structure were identified through small vibration amplitude tests and are provided in Table 1 for the three-story structure. As mentioned previously and demonstrated in Table 1, the addition of fluid dampers had a primary effect of increasing damping while stiffening the higher modes.

The scale model building was subjected to earthquake motion at the base using the large earthquake simulator located at the National Center for Earthquake Engineering Research in Buffalo, NY. The following earthquake records were used in the testing program: 1) El Centro record (comp. S00E) of the 1940 Imperial Valley earthquake; 2) Taft record (comp. N21E) of the 1952 Kern County earthquake; 3) Pacoima record (comp. S74W) of the 1971 San Fernando earthquake; 4) Miyagi-Ken-Oki record (comp. EW) of the 1978 Tohoku University earthquake; and 5) Hachinohe record (comp. NS) of the 1968 Tokachi-Oki earthquake. The earthquake records were selected to provide input motion having a variety of characteristics in terms of, for example, magnitude, predominant frequency range, and peak

acceleration. In this paper, selected results are provided for the first three earthquake records listed above.

Table 1: Identified Properties of Three-Story Model Structure.

Frequency and Damping Ratio	Mode 1	Mode 2	Mode 3
No Dampers	2.00 Hz 1.74 %	6.60 Hz 0.76 %	12.20 Hz 0.34 %
2 Dampers	2.03 Hz 9.9 %	6.88 Hz 14.7 %	12.34 Hz 5.0 %
4 Dampers	2.11 Hz 17.7 %	7.52 Hz 31.9 %	12.16 Hz 11.3 %
6 Dampers	2.03 Hz 19.4 %	7.64 Hz 44.7 %	16.99 Hz 38.0 %

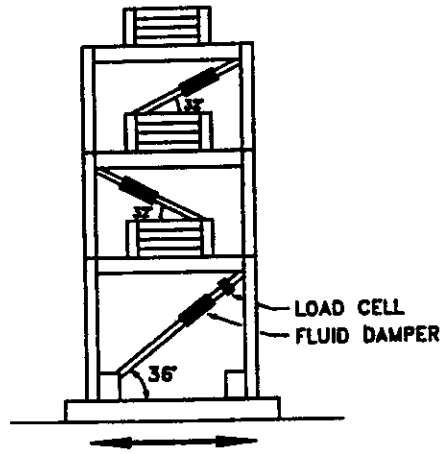

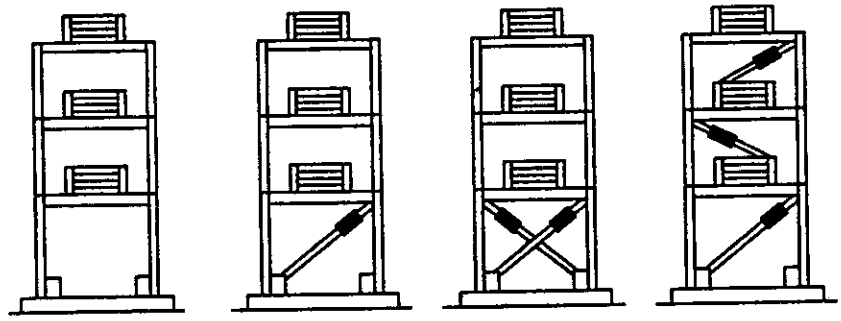

Fig. 7 Three-story model structure and damper configurations

1. Energy Response-Histories

The effect of fluid dampers on the behavior of the structure may be vividly illustrated in graphs of the response-history of the energy dissipated by various mechanisms in the structure. For the one-story structure, the energy quantities within the conservation of energy relationship given by Equation (1) can

be calculated as follows. The absolute input energy at time t is the integral of the base shear over the ground displacement and may be written as

$$E(t) = \int_0^t m[\ddot{u}(t) + \ddot{u}_g(t)]\, du_g(t) \tag{5}$$

where m is the mass of the structure, u is the relative displacement of the structure, u_g is the ground displacement, and the double overdots indicate second-order differentiation with respect to time. The absolute kinetic energy is given by

$$E_k(t) = \frac{1}{2} m[\dot{u}(t) + \dot{u}_g(t)]^2 \tag{6}$$

The recoverable strain energy may be written as

$$E_s(t) = \frac{1}{2} k[u(t)]^2 \tag{7}$$

where k is the linear elastic stiffness of the structure. The energy dissipated by the fluid dampers is given by

$$E_d(t) = \int_0^t P_d(t)\, du(t) \tag{8}$$

where P_d is the total damper force acting to resist the motion of the structure. Finally, the irrecoverable energy dissipated by other mechanisms in the structural frame, $E_h(t)$, is evaluated from Equation (1) using the results from Equations (5) through (8).

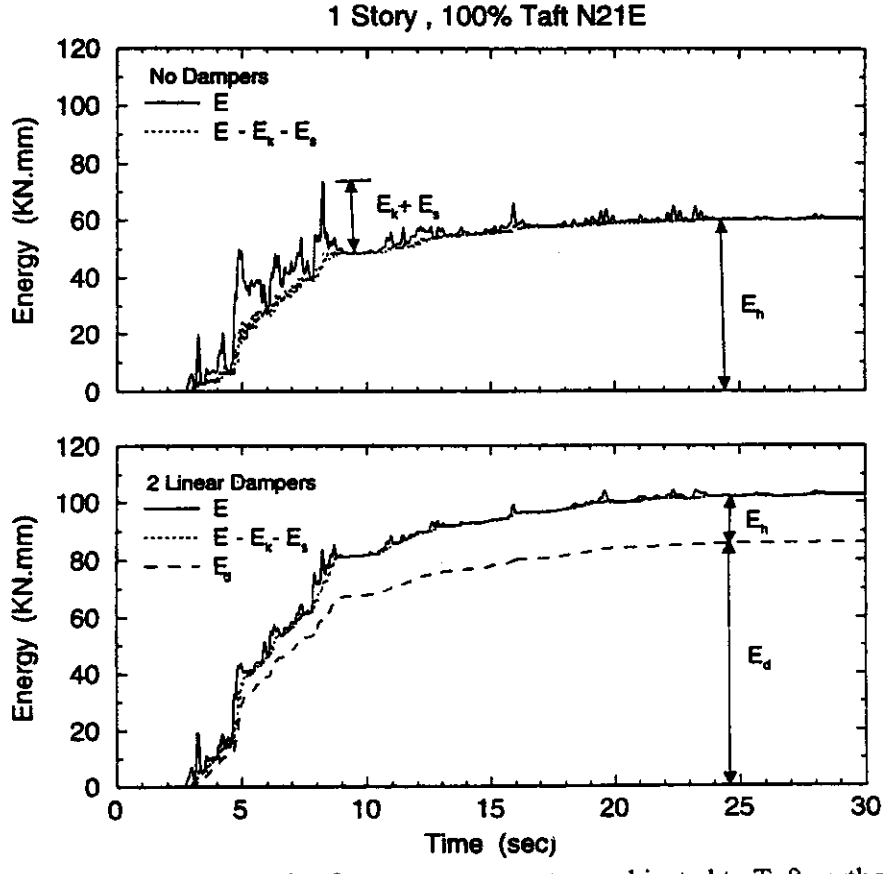

Fig. 8 Energy time-histories for one-story structure subjected to Taft earthquake

Figure 8 shows energy response-histories for the one-story structure subjected to the Taft record (component N21E) of the 1952 Kern County earthquake. The top plot is for the bare frame structure (i.e., no dampers attached) and the bottom plot is for the structure with two fluid dampers attached. As demonstrated in Figure 8, the addition of fluid dampers resulted in an increase in the absolute input energy. This is not surprising since at the end of the earthquake the absolute energy input must equal the energy dissipated in the system. Therefore, it is expected that the structure with two dampers attached (damping ratio of about 16 %) would have a large absolute input energy at the end of the earthquake. In contrast, for the bare frame structure with its relatively low inherent damping (damping ratio of about 2.5 %), the ability to dissipate energy is low which results in a small absolute input energy at the end of the earthquake. A more detailed explanation of this phenomenon is presented in the work by Seleemah and Constantinou (1997). It is important to recognize that the energy quantities of relevance to the seismic behavior of a structure are the sum of the kinetic and strain energies, $E_k + E_s$, which indicate the level of deformation in the structure, and the irrecoverable energy dissipated by the structural frame, E_h, which indicates the level of inelastic action in the structure. It is clear from Figure 8 that the addition of energy dissipating devices to the test structure results in a reduction of both of these energy quantities and thus improves the seismic performance of the structure. In particular, one may note the significant reduction of energy dissipated in the structural frame, E_h, in exchange for energy dissipation by the fluid dampers, E_d.

2. Peak Response Reduction

The benefit of including fluid dampers can also be demonstrated by examining peak response profiles. Figure 9 shows response profiles of the three-story structure subjected to the El Centro record (component S00E) of the 1940 Imperial Valley earthquake. One profile is for the case of no dampers and the earthquake record scaled in magnitude by 1/3. The other profile is for the case of six dampers and the unscaled earthquake record. Recall that the damping ratio of the fundamental mode is about 2 % for the bare frame structure and about 19 % for the frame with six fluid dampers (see Table 1). Evidently, the responses of the two systems are approximately the same for two significantly different levels of the same earthquake. For this particular set of tests, the addition of fluid dampers increased the earthquake resistance of the structural frame by three-fold. Of course, this is not generally the case. The reduction achieved by increasing the damping ratio depends on the period of the structure and the frequency content of the excitation.

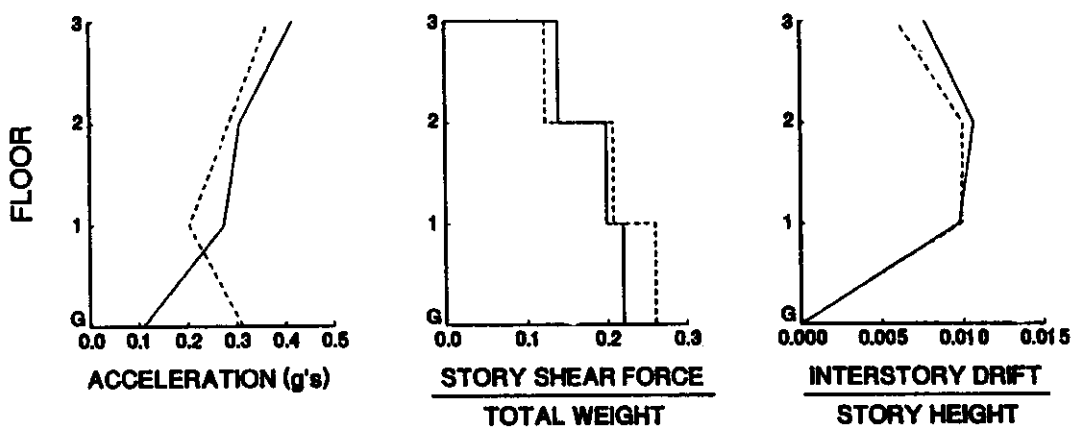

Fig. 9 Comparison of peak response profiles for two different levels of the same earthquake

In general, the inclusion of fluid viscous dampers (i.e., two, four or six dampers) in the structural frame resulted in reductions in story drifts of 30 % to 70 %. These reductions are comparable to those achieved by other energy dissipating systems such as viscoelastic, friction and hysteretic dampers (Aiken and Kelly, 1990; Whittaker et al., 1989). However, the use of fluid dampers also resulted in reductions of story shear forces by 30 % to 60 %, while other energy absorbing devices were incapable of achieving any comparable reduction. The reason for this difference is the essentially pure linear viscous behavior of the tested fluid dampers which results in an out-of-phase relationship between the column restoring forces and the fluid damper forces.

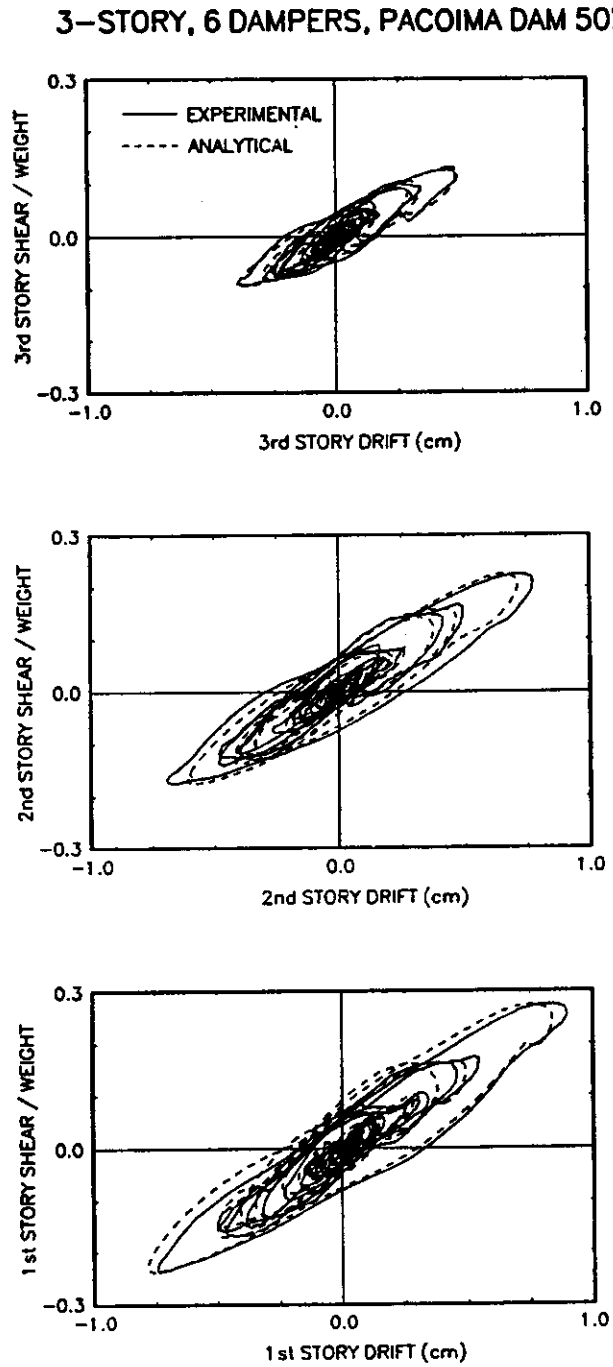

Fig. 10 Comparison of experimental and analytical results for three-story structure with six dampers subjected to Pacoima dam earthquake

3. Analytical Predictions

Comparisons of analytical and experimental story shear force versus story drift loops for the three-story model structure with six fluid dampers subjected to the Pacoima Dam record (component S74W) of the 1971 San Fernando earthquake are presented in Figure 10. Note that the earthquake record was scaled in magnitude by 50 %. The analytical results were obtained through response-history analysis in which the model structure was idealized as a lumped mass system. The stiffness and damping matrices were identified using experimentally obtained natural frequencies, damping ratios and mode shapes. The damper behavior was modeled according to the classical Maxwell model described by Equation (2). The comparisons shown in Figure 10 demonstrate the validity of the analytical model of the fluid dampers and structural frame. Note that similar agreements between analytical and experimental results were obtained for the structure outfitted with two or four dampers.

GENERALIZED FLUID VISCOUS DAMPERS

The linear viscous damper model of Equation (4) may be written in a generalized form as follows

$$P(t) = C_o \left|\dot{u}(t)\right|^{\alpha} \operatorname{sgn}\left[\dot{u}(t)\right] \tag{9}$$

where α is a real positive exponent with typical values in the range of 0.5 to 2. The value of the exponent is primarily controlled by the design of the piston head orifices. Note that when α is equal to unity, Equation (9) collapses to the linear viscous dashpot model as given by Equation (4). Further, when α is not equal to unity, the behavior of the damper is nonlinear. Specifically, when the piston head orifices are cylindrical, α = 2 and the output force is proportional to velocity squared. Such damping is known as square law or Bernoulli damping. The performance of such dampers is typically unacceptable for seismic energy dissipation. To produce damping forces with exponent α different than 2 requires specially shaped orifices to alter the flow characteristics with fluid speed. As described in Section 3, the resulting orifice design is known as a fluidic control orifice. A design with exponent α equal to 0.5 is useful in applications involving extremely high velocity shocks such as shock isolation of military hardware or seismic protection of structures located in the forward rupture directivity region of near-fault earthquakes. The ground motion associated with such near-fault earthquakes is typically characterized by large low-frequency velocity (on the order of 1 m/s or more) and displacement (on the order of 0.5 m or more) pulses. Fluid viscous dampers with nonlinear characteristics have been specified in a number of projects in the U.S. For example, the Arrowhead Regional Medical Center in Colton, California is a five building base-isolated complex utilizing 400 high damping rubber bearings and 186 nonlinear fluid viscous dampers with α = 0.5 (Asher et al., 1996). Furthermore, studies on the seismic retrofit of the suspended part of the Golden Gate bridge in San Francisco concluded that the use of fluid dampers with α = 0.75 produce the desired performance (Rodriquez et al., 1994).

ENERGY DISSIPATION CHARACTERISTICS OF FLUID VISCOUS DAMPERS

The frequency-dependent energy dissipation characteristics of fluid dampers may be described by considering the response of the damper to an imposed harmonic displacement. The harmonic displacement is most simply described by

$$u = u_o \sin(\omega t) \tag{10}$$

where u_o is the amplitude of displacement and ω is the circular frequency of motion. The energy dissipated during the harmonic motion is obtained by integrating the damper output force over the imposed displacement. For a single cycle of motion, the energy dissipated may be written as

$$E_d = \oint P(t)du(t) = \int_0^T P(t)\dot{u}(t)dt \tag{11}$$

where T is the period of the harmonic motion.

For the case of the generalized fluid damper behavior given by Equation (9), the energy dissipation per cycle is given by

$$E_d = \int_0^T C_o |\dot{u}|^\alpha \dot{u} \operatorname{sgn}(\dot{u}) dt \tag{12}$$

which may be evaluated by contour integration in the complex plane. The result is as follows

$$E_d = \frac{4C_o(2\omega)^\alpha (u_o)^{\alpha+1} \Gamma^2\left(1+\frac{\alpha}{2}\right)}{\Gamma(2+\alpha)} \tag{13}$$

where Γ is the gamma function. The energy dissipated may also be written in terms of the maximum damper force, P_{max}, as follows

$$E_d = \frac{4P_{max} u_o (2^\alpha) \Gamma^2\left(1+\frac{\alpha}{2}\right)}{\Gamma(2+\alpha)} \tag{14}$$

where $P_{max} = C_o(u_o\omega)^\alpha$. The differences in energy dissipation characteristics of linear and nonlinear fluid dampers may now be evaluated using Equation (14). For linear dampers, α = 1 and E_d = $3.142 P_{max} u_0$. For nonlinear dampers with α = 0.5 (a technologically advanced design with fluidic orifices), E_d = $3.496 P_{max} u_0$ and when α = 2 (a simple design with cylindrical orifices), E_d = $2.667 P_{max} u_0$. Thus, for the same level of maximum force and amplitude of motion, the nonlinear damper with α = 0.5 dissipates 11 % more energy per cycle than the linear damper with α = 1 and 31 % more than the nonlinear damper with α = 2.

The significance of this difference in energy dissipation can be conveniently demonstrated by evaluating the behavior of a single-degree-of-freedom system with mass m, linear elastic stiffness k, and a single damper with characteristics defined by Equation (9). The damping ratio of the system may be expressed as (Chopra, 1995)

$$\xi = \frac{E_d}{4\pi E_s} = \frac{E_d}{2\pi k u_o^2} \tag{15}$$

where E_s is the elastic energy stored at the maximum displacement, u_o. Substituting Equation (13) into Equation (15) results in

$$\xi = \frac{2^{\alpha+1} u_o^{\alpha-1} \omega^{\alpha-2} C_o}{\pi m} \frac{\Gamma^2\left(1+\frac{\alpha}{2}\right)}{\Gamma(2+\alpha)} \tag{16}$$

where now ω represents the undamped natural circular frequency of the structural system. For a linear fluid damper, we have

$$\xi_{\alpha=1} = \frac{C_o}{2m\omega} \tag{17}$$

and for a nonlinear fluid damper with α = 0.5

$$\xi_{\alpha=0.5} = 0.55641 \frac{C_o}{m\sqrt{u_o \omega^3}} \tag{18}$$

and for a nonlinear fluid damper with α = 2

$$\xi_{\alpha=2} = \frac{4C_o u_o}{2\pi m} \tag{19}$$

As expected, the damping ratio is generally dependent on the amplitude of motion. For nonlinear dampers with α < 1, the damping ratio reduces with increasing amplitude of motion. The opposite is true for nonlinear dampers with α > 1. For the linear case (α = 1), the damping ratio is independent of

the amplitude of motion. The dependency of the damping ratio on the amplitude of motion is demonstrated in Figure 11 which shows the damping ratio of a single-degree-of-freedom system with a weight of 7000 kN and an undamped natural frequency of π rad/sec. Three different damper configurations are considered, each of which produces a maximum damper force of 704 kN (10 % of the weight) at a velocity of 785 mm/sec. For the linear damping case, the damping constant, C_o, is equal to 0.8967 kN-sec/mm whereas for the nonlinear damping cases, the damping constant is equal to 25.13 kN-sec$^{1/2}$/mm$^{1/2}$ for $\alpha = 0.5$ and 0.001142 kN-sec^2/mm^2 for $\alpha = 2$. Note from Figure 11 that the damping ratio of the nonlinear system with $\alpha = 0.5$ approaches infinity as the amplitude of motion tends to zero. In reality, at low values of velocity, actual devices exhibit linear behavior such that the damping ratio levels off to a constant value as shown by the dashed line in the figure.

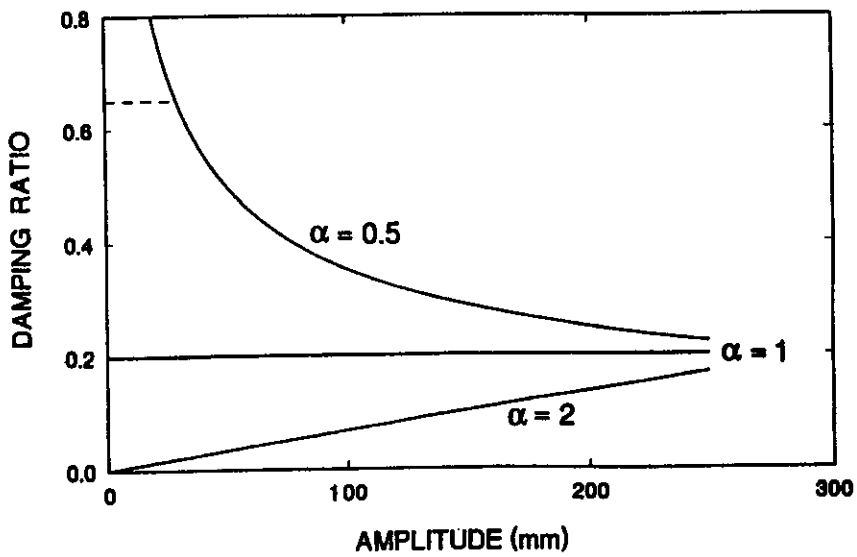

Fig. 11 Damping ratio of systems with nonlinear fluid dampers as a function of amplitude of motion

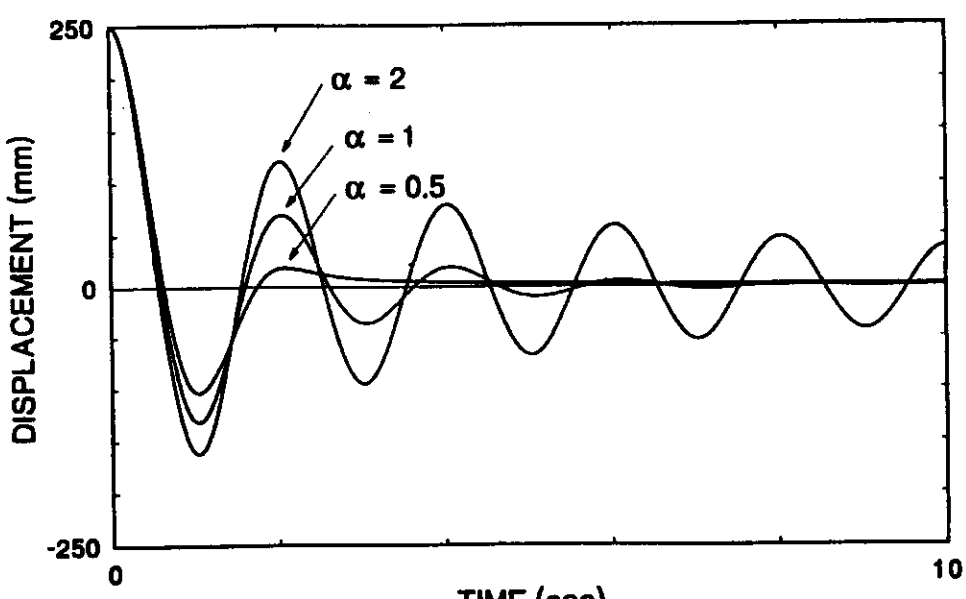

Fig. 12 Response-histories of motion of single-degree-of-freedom system with nonlinear fluid dampers when released from an initial displacement

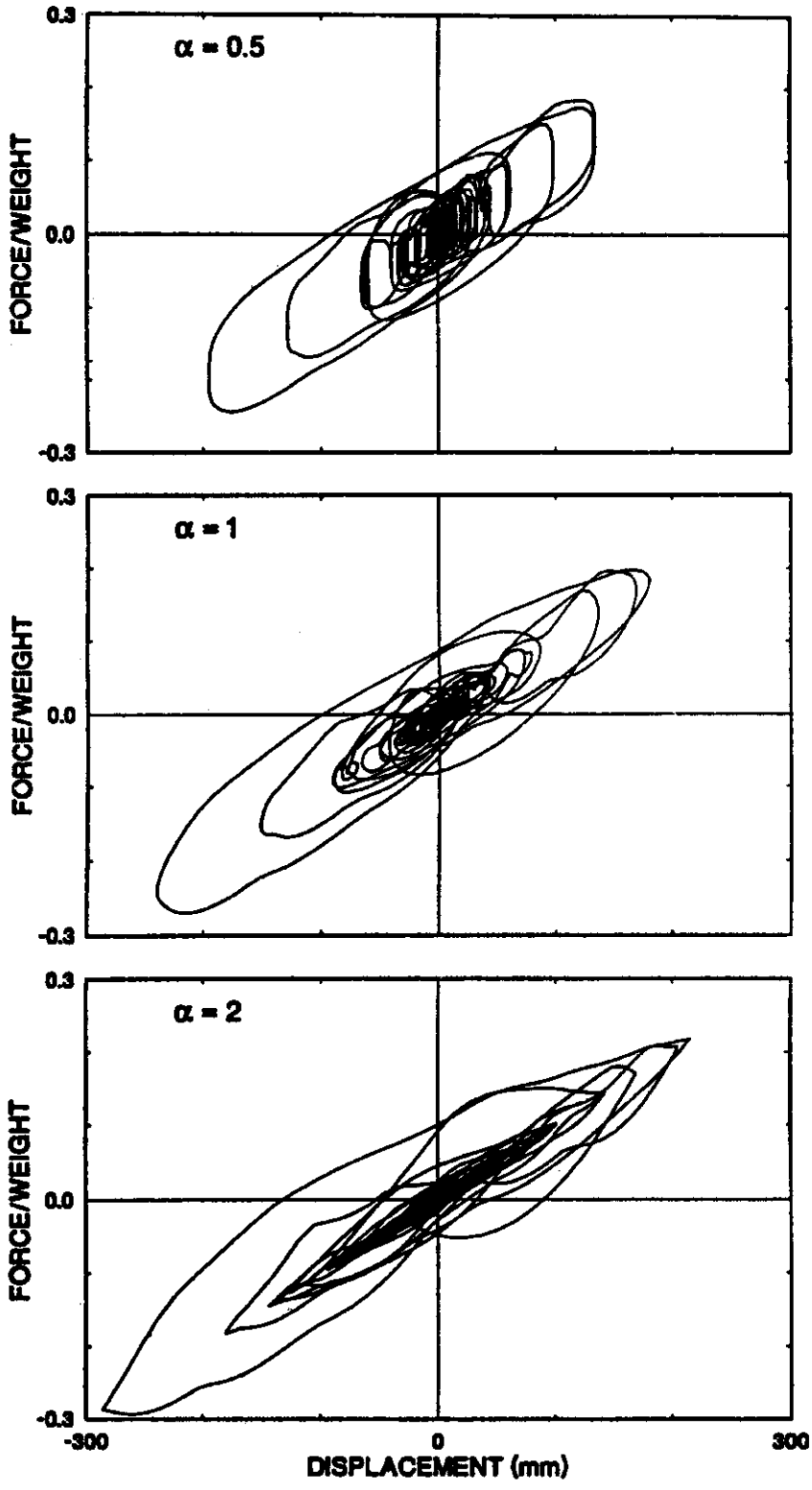

Fig. 13 Force-displacement loops of response of systems with nonlinear fluid dampers when subjected to the El Centro earthquake

The behavior of the three different single-degree-of-freedom systems described above under free vibration and seismic excitation is shown in Figures 12 and 13, respectively. In Figure 12, the displacement response-histories of the three systems are compared when they are released from an initial

Table 2 (cont.): Chronological Listing of Structural Applications of Fluid Dampers for Seismic Hazard Mitigation

Name of Structure	Location	Number, Output Force and Stroke	Date of Installation	Additional Information
The Money Store National Headquarters	Sacramento, California	120, 710 kN, ±64 mm 1290 kN, ±64 mm	1996	New construction, pyramid shaped 11-story building, moment-frame structure, dampers in diagonal braces.
Quebec Iron and Titanium Smelter	Canada	22, 450 kN, ±64 mm 225 kN, ±100 mm 130 kN, ±100 mm	1997	Dual purpose spring dampers for seismic and wind protection of two buildings. Dampers prevent building impact during a seismic event.
Hayward City Hall	Hayward, California	15, 1400 kN, ±600 mm	1997	New construction, dampers in base isolation system.
Rockwell Building 505	Newport Beach, California	6, 320 kN, ±64 mm	1997	Retrofit of building with multiple expansion gaps. Dampers restrict relative movement between building sections.
CSULA Administration Building	Los Angeles, California	14, 1100 kN, ±75 mm	1997	Seismic upgrade of office building, dampers in chevron bracing.
San Francisco Civic Center	San Francisco, California	292, 1000 kN, ±100 mm 550 kN, ±100 mm	1997	New construction, 14-story office building, dampers in diagonal bracing.
Alaska Commercial Building	Alaska	2, 445 kN, ±64 mm	1997	Retrofit of timber frame structure, dampers in diagonal bracing.
Studio Parking Garage	Los Angeles, California	2, 150 kN, ±50 mm	1997	Dampers allow thermal motion, concrete expansion/contraction and creep, while controlling earthquake movement.
UCLA-Knudsen Hall	Los Angeles, California	84, 355 kN, ±100 mm 245 kN, ±100 mm	1998	Seismic upgrade of University building. Dampers in chevron bracing.
New Pacific Northwest Baseball Park	Seattle, Washington	36, 1780 kN, ±100 mm 890 kN, ±400 mm	1998	New baseball stadium, dampers dissipate seismic energy in each of three movable roof sections.
Tillamook Hospital	Tillamook, Oregon	30, 150 kN, ±50 mm	1998	Retrofit of existing hospital. Dampers in chevron bracing.
San Francisco-Oakland Bay Bridge, East Span	San Francisco, California	6, 890 kN, ±406 mm	To be installed 1999	Interim retrofit of East Bay 504 truss sections.
1414 K Street	Sacramento, California	8, 1125 kN, ±63 mm	To be installed 1999	Retrofit of existing office building. Dampers in diagonal bracing.

displacement of 250 mm. The differences in energy dissipation capacity of the three systems are evident in the reduction of amplitude per cycle of motion. In Figure 13, the force-displacement loops of the three systems are compared for the case of seismic excitation due to the El Centro record (component S00E) of the 1940 Imperial Valley earthquake scaled in magnitude by a factor of two. Note that the force in Figure 13 is the total column shear force (i.e., restoring force plus damper force). The better performance of the system with a nonlinear damper (α = 0.5) is apparent. In comparing the performance of the nonlinear system (α = 0.5) with the linear system, we observe a nearly 20 % reduction in displacement and a 10 % reduction in total force. This better performance of the system with α = 0.5 is achieved with a peak damper force that is less than that of the other systems. Specifically, for α = 0.5 the peak damper force is 640 kN, whereas for α = 1 and α = 2 the peak damper force is 700.5 kN and 930.5 kN, respectively.

APPLICATIONS OF FLUID DAMPER SYSTEMS FOR SEISMIC PROTECTION

In addition to the research described herein, a number of experimental studies have been performed on structures incorporating fluid dampers for seismic energy dissipation. For example, seismic simulation tests have been performed on a seismically-isolated 1/4-scale bridge model (Tsopelas et al., 1996), a seismically-retrofitted 1/3-scale reinforced concrete building model (Reinhorn et al., 1995), a 1/4-scale building model with both linear and nonlinear fluid dampers (Seleemah and Constantinou, 1997) and a 1/2-scale stiff steel building frame with a toggle-brace-damper system to magnify the damping effect (Constantinou et al., 1997). These experimental studies have verified the suitability of fluid dampers for seismic protection of structures and thus have led to a number of completed and pending applications. Passive fluid viscous damping systems have been installed or are scheduled for installation in at least 30 major buildings and bridge structures within seismically active regions of the U.S. (see Table 2). Two applications to building structures are discussed below; one application within the seismic lateral force resisting system of the structure and one application within a seismic base-isolation system. Note that practical seismic fluid viscous dampers are available with force and displacement capacities that range from approximately 50 kN to 9000 kN and ±1 to ±125 cm, respectively.

Table 2: Chronological Listing of Structural Applications of Fluid Dampers for Seismic Hazard Mitigation

Name of Structure	Location	Number, Output Force and Stroke	Date of Installation	Additional Information
Pacific Bell North Area Operation Center	Sacramento, California	62, 130 kN, ± 50 mm	1995	New construction, 3-story steel braced frame, dampers in chevron bracing.
Langenbach House	Oakland, California	4, 130 kN, ± 150 mm	1996	Dampers in base isolation system.
CSUS Science II Building	Sacramento, California	40, 220 kN, ± 50 mm	1996	New structure, dampers in chevron bracing.
Arrowhead Regional Medical Center (5 buildings)	San Bernardino, California	186, 1400 kN, ± 610 mm	1996	New construction, dampers in base isolation system.
Hotel Woodland	Woodland, California	16, 450 kN, ± 50 mm	1996	Retrofit of 4-story historic masonry structure, dampers in chevron bracing.
Kaiser Data Center	Corona, California	16, 425 kN, ± 560 mm	1996	Retrofit, dampers in base isolation system.

Table 2 (cont.): Chronological Listing of Structural Applications of Fluid Dampers for Seismic Hazard Mitigation

Name of Structure	Location	Number, Output Force and Stroke	Date of Installation	Additional Information
Sidney Lanier Bridge	Glynn County, Georgia	4, 2200 kN, ±203 mm	To be installed 1999	New bridge, dampers control earthquake movement and distribute forces while allowing free thermal movement.
I-5/91 HOV Bridge	Anaheim, California	8, 1110 kN, ±200 mm	To be installed 1999	New bridge, dampers dissipate earthquake energy to reduce demand on structure.
San Francisco International Airport - South International Parking Garage Pedestrian Bridge	San Francisco, California	20, 445 kN, ±254 mm	To be installed 1999	New pedestrian bridge, dampers dissipate earthquake energy and control movement
San Francisco International Airport - Rail Transit System Westside Guideway	San Francisco, California	10, 4225 kN, ±508 mm 3115 kN, ±508 mm	To be installed 1999	New Airport Rail Transit (ART) and Bay Area Rapid Transit (BART) structure, dampers dissipate seismic energy.
Cape Girardeau Bridge	Cape Girardeau, Missouri	8, 6700 kN, ±180 mm	To be installed 1999	New construction, cable-stayed bridge. Dampers control earthquake movement while allowing free thermal movement.
Los Angeles City Hall	Los Angeles, California	68, 1400 kN, ±600 mm 1000 kN, ±115 mm	To be installed 1999	Retrofit of City Hall building, dampers in base isolation system. Also uses dampers at 27th floor to protect tower.
Rio Vista Bridge	Rio Vista, California	8, 685 kN, ±254 mm	To be installed 1999	Retrofit of highway bridge.
Maysville Bridge	Maysville, Kentucky	8, 1300 kN, ±305 mm	To be installed 1999	New bridge, dampers control earthquake movement and distribute forces while allowing free thermal movement.
Willamette River Pedestrian Bridge	Eugene, Oregon	4, 500 kN, ±40 mm	To be installed 1999	Retrofit of bridge over Willamette River. Dampers control wind and seismic motion while allowing free thermal movement.
Santa Clara Police Facility	Santa Clara, California	40, 575 kN, ±25 mm 800 kN, ±25 mm	To be installed 1999	New police facility. Dampers in chevron bracing.

Table 2 (cont.): Chronological Listing of Structural Applications of Fluid Dampers for Seismic Hazard Mitigation

Name of Structure	Location	Number, Output Force and Stroke	Date of Installation	Additional Information
Transbay Transit Terminal	San Francisco, California	36, 1300 kN, ±44 mm 1300 kN, ±76 mm	To be installed 1999	Retrofit of bus terminal. Dampers in chevron bracing.
Beijing Railway Station	Beijing, China	32, 1300 kN, ±44 mm	To be installed 1999	Retrofit of railway station. Dampers in chevron bracing.
Triborough Bridge Approaches	New York, New York	80, 445 kN, ±152 mm	To be installed 2000	Retrofit of approaches to suspension bridge. Dampers control earthquake movement and distribute forces while allowing free thermal movement.
Chapultepec Tower	Mexico City, Mexico	98, 5600 kN, ±52 mm 2770 kN, ±52 mm	To be installed 2000	New high-rise office/hotel tower uses dampers in mega-braces.

The Money Store National Headquarters in Sacramento, California is an 11-story, 42,000 m^2, pyramid-shaped office building (Miyamoto and Scholl, 1997). The lateral force resisting system of the building consists of steel moment-resisting frames with linear fluid viscous dampers attached to the frames in a chevron bracing arrangement. For the design basis earthquake, the structure is expected to remain elastic with story drift ratios limited to 0.5 % to protect the welded steel moment connections. A total of 120 fluid viscous dampers were installed in the structure in 1996. Two different damper types were installed, one having a force and displacement capacity of 710 kN and ± 64 mm, respectively, and the other having capacities of 1290 kN and ± 64 mm, respectively.

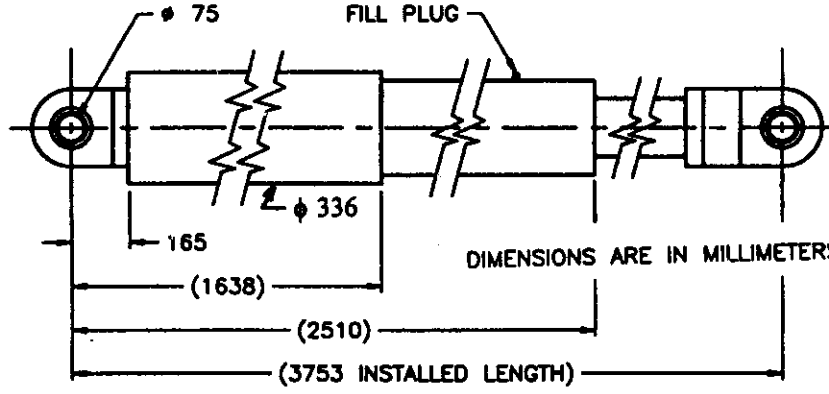

Fig. 14 Construction of nonlinear fluid damper for the Arrowhead Regional Medical Center

Passive fluid viscous dampers with nonlinear characteristics have been installed within the seismic isolation system of the Arrowhead Regional Medical Center in Colton, California (Asher et al., 1996). The Center is a five building complex with a base isolation system consisting of 400 high damping rubber bearings and 186 nonlinear viscous dampers. The structure is located 3 km from the San Jacinto fault and 10 km from the San Andreas fault. Thus, the design ground motion for the site is very severe. Figure 14 shows the construction of the nonlinear viscous dampers. These dampers have an output force of 1400 kN at a velocity of 1500 mm/s and a stroke of ± 610 mm. Scaled versions of these dampers (scale of 1/6) have been tested at the State University of New York at Buffalo. Figure 15 shows the recorded force-velocity data for one of the tested dampers. The nonlinear characteristics of the damper are evident. It may be noted in this figure that the output of the device is nearly unaffected by

temperature in the range of 0°C to 50°C. This temperature insensitivity was a specific project requirement. It has been achieved entirely by passive means, that is by compensation of the changes in fluid properties with changes in the volume of the fluid and metallic parts.

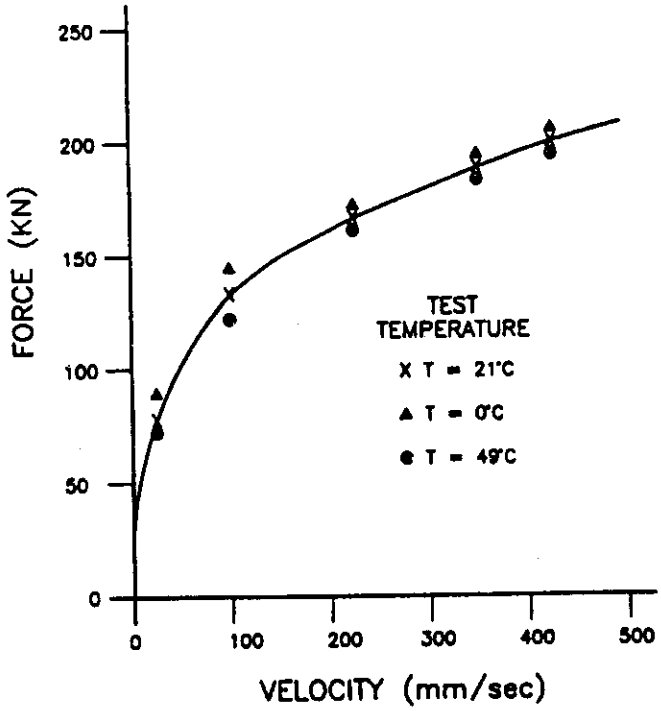

Fig. 15 Force-velocity relationship for 1/6-scale prototype fluid damper of the Arrowhead Regional Medical Center

DESIGN SPECIFICATIONS FOR SEISMIC ENERGY DISSIPATION SYSTEMS

At the present time, the "NEHRP Guidelines for the Seismic Rehabilitation of Buildings" (FEMA, 1997) represents a comprehensive resource document for the analysis and design of buildings with seismic energy dissipation systems. A novelty of these guidelines is the use of displacement-based methods of analysis, a key step towards the application of performance-based seismic design. The analysis and design procedures set forth in the NEHRP Guidelines are not fully developed nor are they fully validated. Studies are currently in progress to extend and validate these procedures.

CONCLUDING REMARKS

Passive fluid viscous damping systems which operate on the principle of fluid orificing are capable of absorbing significant amounts of seismic energy. This has been clearly demonstrated through experimental seismic simulation studies on a scale-model, three-story moment-resisting building frame. The fluid dampers produced simultaneous reductions in story shear forces and story drifts in the structure. Further, it was shown that the use of fluid dampers resulted in a redistribution of energy within the structure such that a large portion of the earthquake energy was absorbed by the dampers rather than by hysteretic action in the structural frame. Mathematical models for defining the dynamic response of the fluid dampers were presented and analytical predictions of the seismic response of the scale-model building structure containing such dampers demonstrated the validity of the models. The energy dissipation characteristics of generalized fluid dampers were analytically evaluated and the benefit of nonlinear behavior for seismic protection of a simple single-degree-of-freedom system was demonstrated. A discussion of current applications of fluid dampers for seismic protection of building and bridges was presented including a description of existing guidelines for the analysis and design of structures with supplemental energy dissipation systems. The future inclusion of such guidelines within

the model building codes will encourage further implementation of supplemental seismic energy dissipation systems.

ACKNOWLEDGEMENTS

Financial support has been provided by the National Center for Earthquake Engineering Research (Project Numbers 90-2101, 93-5120 and 94-5103A) and the National Science Foundation (Grant No. BCS 8857080). Taylor Devices, Inc., N. Tonawanda, NY, manufactured and donated the dampers used in the experiments.

REFERENCES

1. Aiken, I.D. and Kelly, J.M. (1990). "Earthquake Simulator Testing and Analytical Studies of Two Energy-Absorbing Systems for Multistory Structures," Report No. UCB/EERC-90/03, University of California, Berkeley.
2. Arima, F., Miyazaki, M., Tanaka, H. and Yamazaki, Y. (1988). "A Study on Buildings with Large Damping Using Viscous Damping Walls," Ninth World Conf. on Earthquake Engrg., Tokyo, Vol. V, pp. 821-826.
3. Asher, J.W., Young, R.P. and Ewing, R.D. (1996). "Seismic Isolation Design of the San Bernardino County Medical Center Replacement Project," J. of Struct. Design of Tall Buildings, Vol. 5, pp. 265-279.
4. Bird, R.B., Armstrong, R.C. and Hassager, O. (1987). "Dynamics of Polymeric Liquids," Wiley and Sons, New York, NY.
5. Chopra, A.K. (1995). "Dynamics of Structures: Theory and Applications to Earthquake Engineering," Prentice Hall, Englewood Cliffs, New Jersey.
6. Clements, E.W. (1972). "Shipboard Shock and Navy Devices for its Simulation," Report NRL 7396, Naval Research Laboratory, Washington, DC.
7. Constantinou, M.C., Tsopelas, P. and Hammel, W. (1997). "Testing and Modeling of an Improved Damper Configuration for Stiff Structural Systems," Technical Report Submitted to the Center for Industrial Effectiveness and Taylor Devices, Inc.
8. Constantinou, M.C. and Symans, M.D. (1993a). "Experimental Study of Seismic Response of Buildings with Supplemental Fluid Dampers," J. of Struct. Design of Tall Buildings, Vol. 2, pp. 93-132.
9. Constantinou, M.C. and Symans, M.D. (1993b). "Seismic Response of Structures with Supplemental Damping," J. of Struct. Design of Tall Buildings, Vol. 2, pp. 77-92.
10. Constantinou, M.C. and Symans, M.D. (1992). "Experimental and Analytical Investigation of Seismic Response of Structures with Supplemental Fluid Viscous Dampers," National Center for Earthquake Engineering Research, NCEER Report No. 92-0032, State University of New York at Buffalo, Buffalo, NY.
11. FEMA (1997). "NEHRP Guidelines for the Seismic Rehabilitation of Buildings," Report No. FEMA 273, Federal Emergency Management Agency, Washington, DC.
12. Huffman, G.K. (1985). "Full Base Isolation for Earthquake Protection by Helical Springs and Viscodampers," Nuclear Engrg. Design, Vol. 84, No. 2, pp. 331-338.
13. Makris, N., Roussos, Y., Whittaker, A.S. and Kelly, J.M. (1998). "Viscous Heating of Fluid Dampers During Seismic Excitation," Proc. of Fifth Caltrans Seismic Research Workshop, Sacramento, CA.
14. Makris, N. and Constantinou, M.C. (1993). "Models of Viscoelasticity with Complex-Order Derivatives," J. of Eng. Mechanics, Vol. 119, No. 7, pp. 1453-1464.
15. Makris, N. and Constantinou, M.C. (1991). "Fractional Derivative Maxwell Model for Viscous Dampers," J. of Struct. Engrg., ASCE, Vol. 117, No. 9, pp. 2708-2724.

16. Makris, N. and Constantinou, M.C. (1990). "Viscous Dampers: Testing, Modeling and Application in Vibration and Seismic Isolation," National Center for Earthquake Engineering Research, NCEER Report No. 90-0028, State University of New York at Buffalo, Buffalo, NY.
17. Miyamoto, H.K. and Scholl, R.E. (1997). "Design of Steel Pyramid Using Seismic Dampers," Proc. of Structures Congress XV, ASCE, Portland, OR, pp. 1466- 1470.
18. Reinhorn, A.M., Li, C. and Constantinou, M.C. (1995). "Experimental and Analytical Investigation of Seismic Retrofit of Structures with Supplemental Damping: Part 1 - Fluid Viscous Damping Devices," National Center for Earthquake Engineering Research, NCEER Report No. 95-0001, State University of New York at Buffalo, Buffalo, NY.
19. Rodriguez, S., Seim, C. and Ingham, T. (1994). "Earthquake Protective Systems for the Seismic Upgrade of the Golden Gate Bridge," Proc. of Third U.S.-Japan Workshop on Protective Systems for Bridges, Berkeley, CA.
20. Seleemah, A.A. and Constantinou, M.C. (1997). "Investigation of Seismic Response of Buildings with Linear and Nonlinear Fluid Viscous Dampers," National Center for Earthquake Engineering Research, NCEER Report No. 97-0004, State University of New York at Buffalo, Buffalo, NY.
21. Tsopelas, P., Constantinou, M C., Okamoto, S., Fujii, S. and Ozaki, D. (1996). "Experimental Study of Bridge Seismic Sliding Isolation Systems," Engineering Structures, Vol. 18, No. 4, pp. 301-310.
22. Uang, C.M. and Bertero, V.V. (1990). "Evaluation of Seismic Energy in Structures," Earthquake Engrg. and Struct. Dynamics, Vol. 19, pp. 77-90.
23. Whittaker, A.S., Bertero, V.V., Alonso, J.L. and Thompson, C.L. (1989). "Earthquake Simulator Testing of Steel Plate Added Damping and Stiffness Elements," Report No. UCB/EERC-89/02, University of California, Berkeley.